



Enhanced bonded aircraft repair using nano-modified adhesives

G. Gkikas, D. Sioulas, A. Lekatou, N.M. Barkoula, A.S. Paipetis*

Dept. of Materials Science & Engineering, Univ. of Ioannina, 45110 Ioannina, Greece

ARTICLE INFO

Article history:

Received 9 March 2012

Accepted 26 April 2012

Available online 4 May 2012

Keywords:

Bonded repair

Carbon nanotubes

Epoxy

Composites

Galvanic corrosion

ABSTRACT

The scope of the present work is to investigate if the introduction of a small weight fraction of multi wall carbon nanotubes (CNTs) in a polymer adhesive film can: (a) act as an effective corrosion barrier that inhibits access of the electrolyte to the surface of the aluminium substrate thereby preventing or notably delaying destructive localised aluminium corrosion, (b) lead to a hybrid system with galvanically compatible constituents and (c) enhance the adhesion of the film to the alloy substrate. Electrochemical measurements showed that the incorporation of CNTs into the epoxy film does not mediate the galvanic effect between substrate/coating, whilst it introduces limited localised degradation phenomena into the polymer matrix. However, it reduces the uniform corrosion rate of the film. Lap shear testing showed that the adhesion enhancement that stemmed from CNTs doping was significant in the absence of anodising of the substrate. It is proposed that a bi-layer patch, where the intermediate layer will be the neat polymer film and the over-layer will be the CNTs-reinforced film would be beneficial in terms of optimising the anodic protection by the patch and the galvanic compatibility of the alloy substrate/patch system.

© 2012 Elsevier Ltd. All rights reserved.

1. Introduction

The application of bonded composite patches as doublers to repair or reinforce defective metallic structures is becoming recognised as a very effective and versatile method. Various applications of this technology include the repair of cracking, localised reinforcement after removal of corrosion damage and reduction of fatigue strain [1]. Aerospace, automotive, construction, defence and marine are some of the industries that use this technology [2]. Adhesive bonded technology produces plane surfaces without discontinuities and eliminates stress concentrations produced by mechanical fasteners. Co-curing technologies for secondary adhesive bonding also offer distinctive advantages such as: flexibility in shape, easier tooling process and simplified lay-up process [3,4].

The main reason that adhesively bonded patches have been reported to perform better than bolted patches is that the effect of the low shear strength of the adhesive layer is superseded by the large contact area. Edge effects can be minimised with the tapering of the bonded patch. The better efficiency of bonded versus mechanically fastened repair has been clearly demonstrated experimentally [5]. Composite patched aluminium edged notched panels exhibited clearly superior behaviour to fatigue loading, as the crack propagation under the patch was significantly delayed when the doubler was bonded on the substrate [6]. In spite of the above, mechanically fastened patches are usually endorsed by aircraft manufacturers as bonded repair technologies have not yet attained

the required confidence by the aircraft industry for widespread use in structural repair.

As recent research has proven, Carbon Fibre Reinforced Plastics (CFRPs) using CNTs doped matrix material exhibit a spectacular improvement in fracture toughness under mode I and mode II remote loading conditions [7], and significantly higher damage tolerance properties and fatigue life extension [8–10]. Similar results have been published for CNTs modified epoxies, where it was shown that the dispersion conditions are of key importance to obtain improvements in both toughness and thermomechanical properties [11–13]. Only a small weight fraction of CNTs has been reported to improve the mechanical, thermal and electrical properties when dispersed in the matrix of typical aerospace composites [14–17]. The huge interfacial area introduced with CNTs dispersion is also a key factor to the behaviour of the nanocomposite [18]. CNTs are reported to act as plasticisers of the epoxy system [19], as they intervene in the 3D polymer network [12], may be employed to tailor the thermal properties of the patch system in order to minimise the thermal stresses that are present due to the thermal coefficient mismatch between the patch and the parent material [20] and inhibit patch debonding, as they are reported to increase the damage tolerance in typical structural composites. These enhanced properties can be readily exploited in aircraft repair technologies; CNTs are very promising as adhesion enhancers in typical bonded repairs, particularly during dynamic loading.

CNTs may appear ideal in terms of enhancing adhesion or damage tolerance but the question still remains: are they compatible with typical aluminium aircraft structures in terms of galvanic corrosion? Aircraft alloys and especially the two most commonly

* Corresponding author. Tel.: +30 26510 08001; fax: +30 26510 08054.

E-mail address: paipetis@cc.uoi.gr (A.S. Paipetis).

used Al alloys AA 2024 T-3 and AA 7075 T-6 are designed to impart high strength and light weight to aircraft, but are often susceptible to local galvanic corrosion, [21,22], and among the most difficult to protect of all aluminium alloys [23]. Pitting susceptibility of these alloys is strongly associated with their intermetallic inclusions [24]. Information on the corrosion performance of CNTs reinforced composites with when coupled with Aluminium or other metallic substrates is very limited in the literature. Recently, Ireland et al. [25] reported that the presence of multi-wall CNTs in Glass Fibre Reinforced Plastics (GFRPs) promotes galvanic corrosion of Al7075. More specifically, coupling of MWCNT/GFRPs with Al7075 samples caused approximately double corrosion rate and mass loss rate, compared to baseline GFRP samples. However, the incorporation of CNTs into a nickel coating increased its corrosion resistance by filling microscale defects and restricting localised corrosion [26]. Nevertheless, useful information can be found in works including electrochemical measurements to evaluate the protection abilities of conducting polymers and PMCs. According to Angelopoulos [27], the use of conducting polyaniline coatings deposited on Cu and Ag results in protection against galvanic corrosion, as determined by potentiodynamic polarisation measurements in a 3-electrode electrochemical cell.

The scope of this effort is to investigate whether the introduction of a small amount of CNTs into a polymer adhesive film can: (a) act as an effective corrosion barrier that inhibits access of the electrolyte to the surface of the aluminium substrate, thereby preventing or notably delaying destructive localised aluminium corrosion, (b) lead to a hybrid system with galvanically compatible constituents, since both the CNT-doped polymer and the Al-alloy constitute dissimilar conductors when exposed to an electrolyte (c) enhance the adhesion of the film to the alloy substrate and (d) provide a roadmap for the use of polymeric composites reinforced with graphitic elements (e.g. carbon fibres and/or CNTs) for bonded structural repair of ageing aluminium aircrafts).

2. Experimental framework

2.1. Materials and surface treatment

Multi-wall CNTs were incorporated in epoxy at 0.5 wt.% and 1 wt.% using a high shear mixer (2 h at 2250 rpm). The multi-wall CNTs were provided by ARKEMA, France and manufactured by catalysed CVD. Their diameter was 10–15 nm and their length was 500 nm. The resin system was the two component liquid adhesive Epibond 1590 – 3 mm A/B with mix ratio 100/41.5 parts by weight. The unmodified and modified adhesives were employed as coatings on the Al substrates for the electrochemical evaluation or as adhesives for the lap shear testing. Curing was carried out for 2 h at 100 °C. The Supplier of the resin system was Huntsman Advanced Materials, Switzerland.

The substrate used for this study was anodised Aluminium 2024 T3. Surface preparation and anodising was performed in-house, according to the ASTM D3933-98(2010) [28] More analytically, the substrate was sandpapered (100 mesh) for 5 min by hand and cleaned by spraying distilled water and acetone. Afterwards, it was immersed in a sodium hydroxide solution (NaOH) 5% w/w, for 10 min at room temperature and subsequently in distilled water for 5 min at 43 °C. Deoxidation was performed by immersion in a nitric acid solution (HNO₃) 50% w/w for 10 min at room temperature followed by cleaning with distilled water for 5 min at 43 °C by immersion. Anodising was carried out in a phosphoric acid solution (H₃PO₄), 10% w/w for 20 min at room temperature followed by immersion in distilled water for 10 min at 43 °C. Single rack configuration was used, with applied voltage of 10 V for

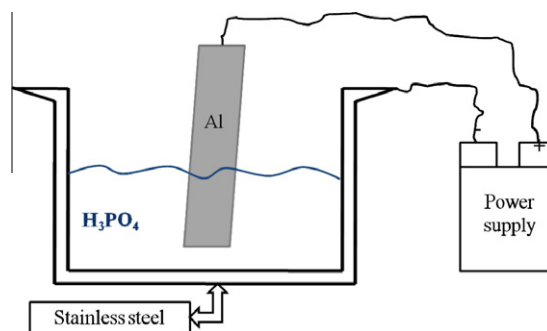


Fig. 1. Anodisation process.

20 min. Finally, the specimens were dried in clean air for 30 min at 80 °C. The experimental configuration is shown in Fig. 1.

2.2. Evaluation techniques

2.2.1. Electrochemical evaluation

Small rectangular coated coupons were cut with a diamond saw, in order to be subjected to electrochemical testing. Ultrasonically cleaned coupons were encapsulated in PTFE, leaving a surface area of ~ 1 cm² to be exposed to aerated 3.5% NaCl, at room temperature (RT). All the electrochemical tests were performed using the Gill AC potentiostat/galvanostat by ACM Instruments. A standard three electrode cell was employed, with Ag/AgCl (3.5 M KCl, $E_{\text{AgCl}} = E_{\text{SHE}} - 200$ mV) as the reference electrode and a platinum gauge as the counter electrode. The electrochemical cell was positioned in a Faraday cage in order to limit interference with the laboratory environment. Potentiodynamic polarisation tests were carried out at a scan rate of 10 mV/min. Reverse polarisation tests were conducted to study the susceptibility of the systems to localised degradation. The rest potential (E_{rest}) was determined after 24 h of immersion in 3.5% NaCl, at room temperature (RT). Corrosion current densities were determined by Tafel extrapolation, as described in a previous work [29].

The galvanic current of anodised Al 2024 T3 with coated anodised Al 2024 T3 was measured. The following coatings were employed: neat epoxy doped with 0.5% CNTs, neat epoxy doped with 1% CNTs. The anodised Al 2024 T3–anodised Al 2024 T3 couple was also studied as a baseline. The galvanic current versus time was continuously recorded by electrically connecting the couple constituents (PTFE masked specimens leaving equal surface areas exposed to the electrolyte) to a zero resistance ammeter (Gill AC by ACM Instruments of current range 10 pA to 500 mA). The Al-alloy was connected to the working electrode 1 (WE₁) input of the galvanostat and the coated substrate to the working electrode 2 (WE₂) (Fig. 2). Should the galvanic current of the couple receive positive values, then WE₁ is anodic to WE₂. The electrolyte provided a means for ion migration, whereby metallic ions moved from the anode to the cathode. Positive current density denoted the movement of the metallic ions from the anode to the cathode. The anode corroded more quickly than if it were on its own in the electrolyte and at the same time, the corrosion of the cathode was retarded or even stopped.

The corroded electrode surfaces were subsequently examined in a JEOL JSM 5600 Scanning Electron Microscope equipped with an EDS (Energy Dispersive Spectrometry) detector.

2.2.2. Effect of CNT incorporation in adhesion efficiency

The effect of CNTs on the adhesion efficiency was studied using the lap shear test, according to the ASTM D5868-01(2008) [30]. Strips of Al 2024 T3 were bonded in a lap configuration employed

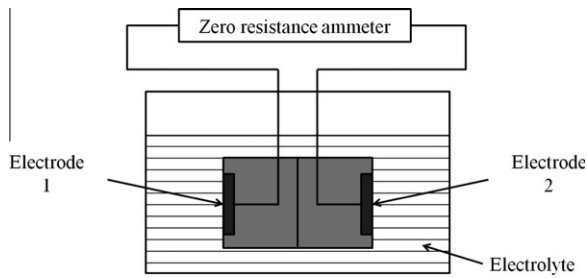


Fig. 2. Experimental arrangement for galvanic corrosion measurements.

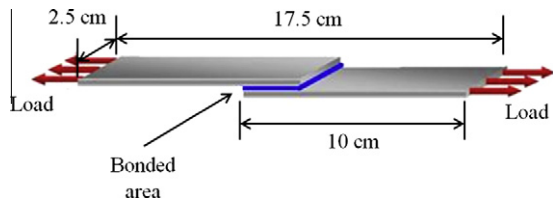


Fig. 3. Coupon for lap shear test.

(i) neat adhesive film and doped adhesive films with (ii) 0.5% CNTs and (iii) 1% CNTs. The dimensions of the manufactured coupons are shown in Fig. 3.

Two different surface preparation protocols were employed for the Al 2024 T3. The first one involved only grinding with 100 mesh sand paper and cleaning with distilled water and acetone (thereafter called untreated). The second one involved additional anodising according to the ASTM D3933-98(2010) [28], (thereafter called treated). After the CNT dispersion in the adhesive, a thin adhesive film was applied on the aluminium surface at a uniform thickness of 1 mm using the blade method and the two aluminium strips were pressured against each other using a vacuum bag. The coupons were subsequently cured according to the cycle provided by the manufacturer and allowed to cool down slowly to room temperature. The bonding strength was obtained using an INSTRON testing machine series 8801 and a Video Extensometer for measuring the axial displacement. The crosshead speed was 13 mm/min.

3. Results and discussion

3.1. Potentiodynamic polarisation

Fig. 4 depicts the polarisation behaviour of all systems immersed in 3.5% NaCl, at room temperature. Fig. 5 presents cyclic polarisation curves for each system. Table 1 lists the extracted electrochemical values. As can be seen in Table 1, doping the adhesive film with CNTs does not bridge the open circuit potential difference and corrosion potential difference between the neat film and Al2024. This result is further investigated by galvanic effect measurements in Section 3.2.

3.1.1. Al2024 T3

As can be seen in Fig. 5a, the Al-alloy, even in the anodised state, was prone to localised corrosion. This was suggested by the following: (a) the abrupt flattening of the gradient in the forward anodic polarisation curve at an overpotential (E_b) of ~ 150 mV higher than the corrosion potential (E_{corr}), indicative of a fast pit propagation which was sustained for more than three orders of magnitude current density increase; (b) the negative hysteresis loop (i.e. higher currents during reverse scanning, as compared with the respective currents during forward scanning), indicative of more active

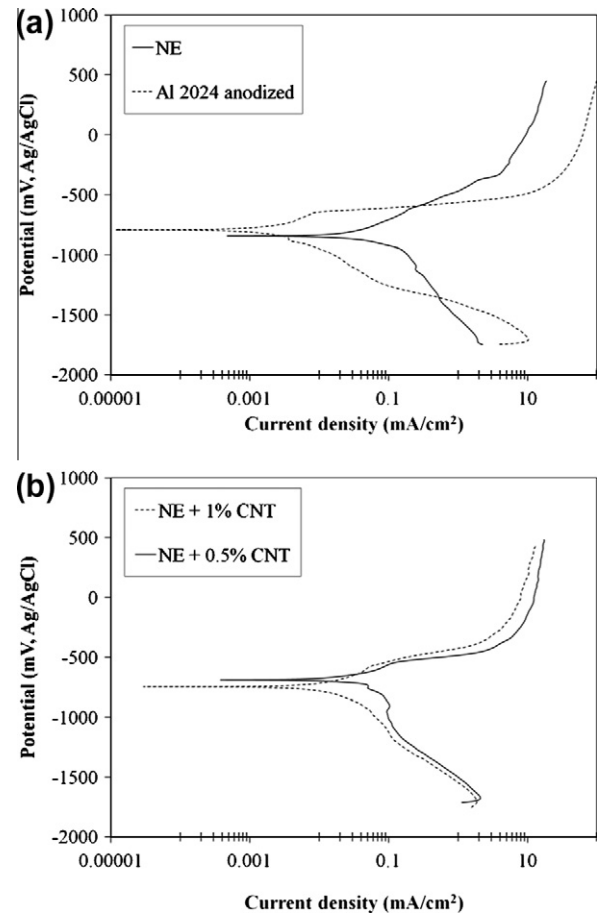


Fig. 4. Potentiodynamic anodic polarisation curves (aerated 3.5% NaCl, R.T.) of (a) epoxy films -neat (NE) and bare anodised Al2024 T3 and (b) 0.5% and 1% p.w. CNT doped- on anodised Al2024 T3.

surfaces during reverse polarisation; (c) the lower anodic-to-cathodic transition (by 64 mV) potential as compared to the corrosion potential indicative of a more active surface.

Even in the case of anodising, the anodic film contained flaws that constituted favoured sites for pit initiation. However, as the measured pitting potential of the alloy was more than ~ 100 mV higher than its corrosion potential (Table 1), anodising had provided protection against pitting. Otherwise, the corrosion potential would have been the same with the pitting potential; as in aerated environments. As is reported in the literature, this is especially the case when the anodic film has deficiently been sealed in order to sustain its ability to anchor organic coatings [31]. The rates of both anodic and cathodic reactions are higher at the flaws and the observed polarisation curves may largely be related to these localised flaws [32]. Al-alloys with flawed passive films, present corrosion potential values equal (or nearly equal) to pitting potential values. This is due to the fact that the cathodic oxygen reduction, largely within the flawed regions, is sufficient to raise the corrosion potential to the pitting potential [33].

3.1.2. Neat epoxy film

Fig. 5b presents the cyclic polarisation behaviour of the neat resin. The conductive behaviour was attributed to the low conductivity of the resin and the water uptake. The distinct differences in the polarisation curves between the neat epoxy film (Fig. 5b) and Al2024 (Fig. 5a) indicated that the electrolyte did not reach the substrate surface. Furthermore, the immersion of neat epoxy coated and uncoated Al2024 specimens in a 3.5% NaCl + 1% Aluminon solution ($C_{22}H_{23}N_3O_9$) for 24 h at room temperature

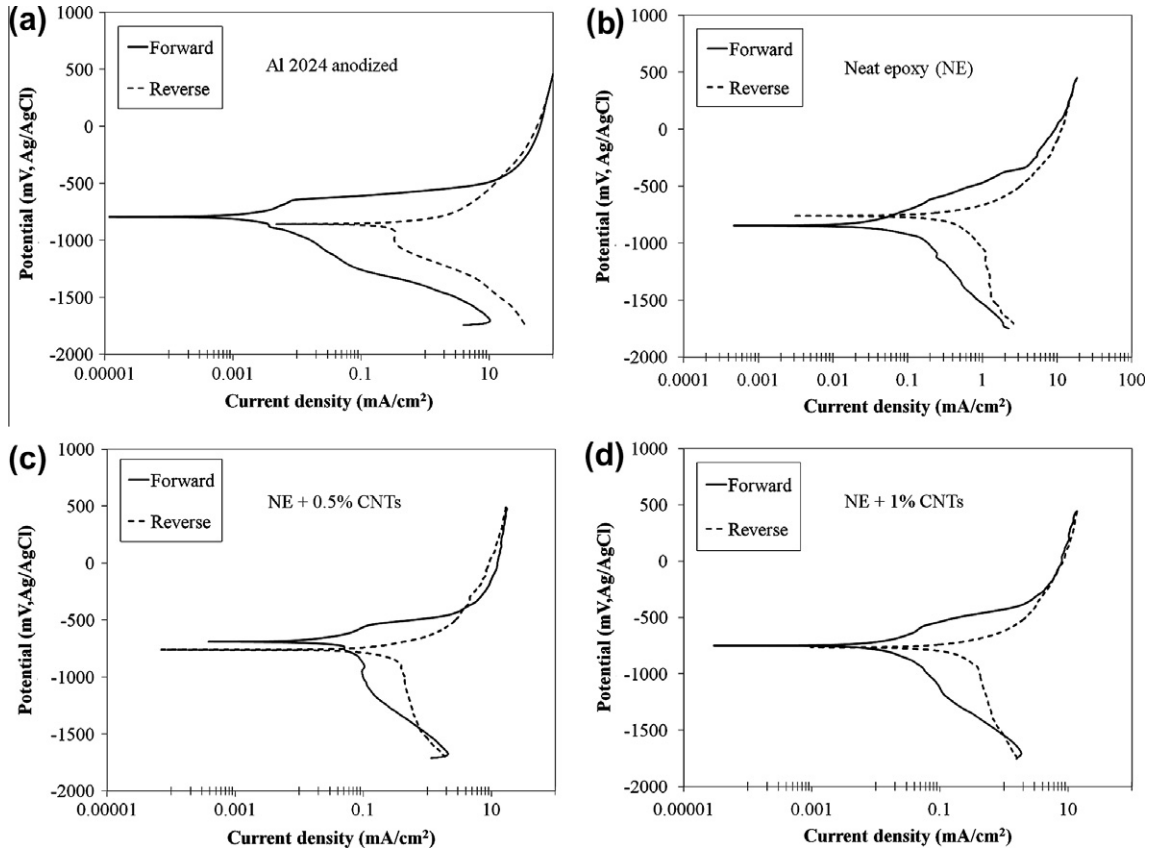


Fig. 5. Cyclic polarisation behaviour of (a) uncoated anodised Al2024 T3, (b) neat epoxy film on anodised Al2024 T3, (c) 0.5 wt.% CNT doped epoxy film on anodised Al2024 T3 and (d) 1 wt.% CNT doped epoxy film on anodised Al2024 T3 (aerated 3.5% NaCl, R.T.).

Table 1

Electrochemical values of the materials immersed in 3.5% NaCl, r.t. E_{rest} , 24 h: open circuit potential after immersion for 24 h. E_{corr} : corrosion potential; E_b : breakaway potential; $E_{a/c/tr}$: anodic-to-cathodic transition potential; i_{corr} : corrosion current density; i_b : current density at E_b .

Material	E_{rest} , 24 h (mV) ^a	E_{corr} (mV)	E_b (mV)	$E_{a/c/tr}$ (mV)	$E_b - E_{corr}$ (mV)	$E_{a/c/tr} - E_{corr}$ (mV)	i_{corr} (mA/cm ²)	i_b (mA/cm ²)
Neat epoxy (NE)	-729	-765	-308 ^b	-682	421	83	0.006	0.18
NE + 0.5% CNT	-689	-689	-558	-762	131	-73	0.002	0.01
NE + 1.0% CNT	-719	-749	-589	-767	160	-18	0.001	0.005
Al2024-T3	-752	-794	-649 ^c	-858	149	-64	0.002	0.009

^a All potential values are cited against the reference Ag/AgCl electrode.

^b The potential value at which a significant abrupt increase in current density is observed.

^c Pitting potential.

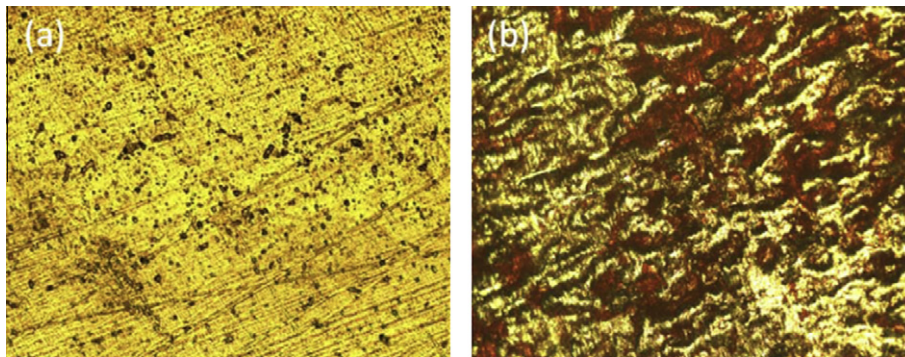


Fig. 6. (a) Surface of coated anodised Al2024 after removing the adhesive film and (b) surface of uncoated anodised Al2024 without adhesive film, both after immersion in 3.5% aerated NaCl + 1% Aluminon solution, for 24 h.

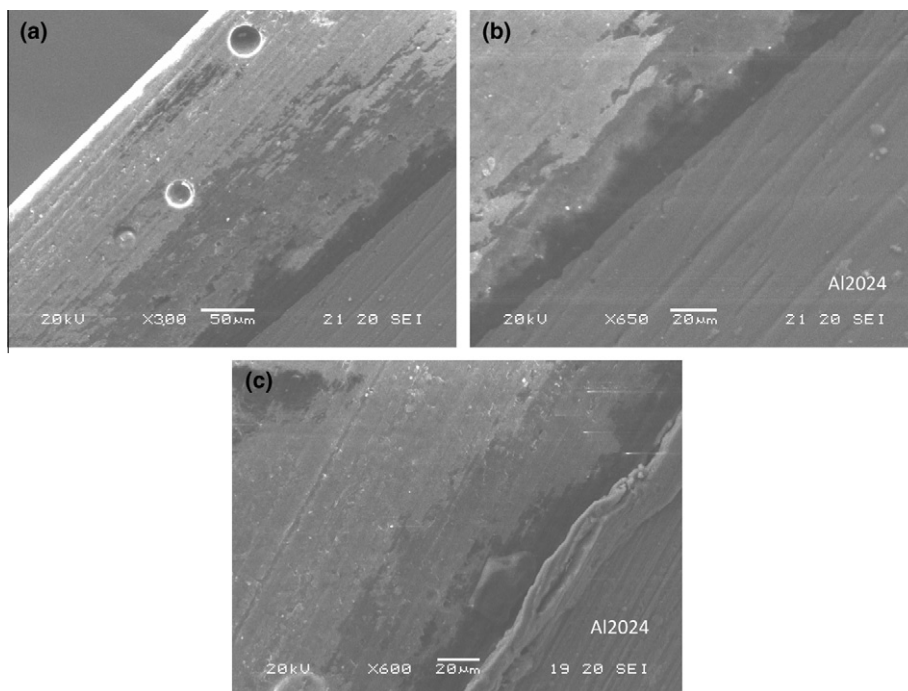


Fig. 7. SEM micrographs of CNT doped coatings on anodised Al2024, after potentiodynamic polarisation (3.5% NaCl, RT), showing that the substrate surface is intact of corrosion. (a) Large – evaporation due – micropores in the coating (0.5% CNTs). (b) 0.5% CNT doped epoxy/Al2024. (c) 1.0% CNT doped epoxy/Al2024; the anodic protection providing film is also discerned on the alloy surface.

(during the recording of the rest potential) revealed that the Al^{3+} ions did not react with Aluminon to form a dye in the case of coated Al (Fig. 6) [34]. The red¹ large spots extensively dispersed on the surface of the uncoated alloy were evident of Al dissolution (Fig. 6a). In contrast, the substrate surface after the removal of the adhesive film did not present any colouration (Fig. 6b), as the electrolyte did not reach the substrate surface during the 24 h immersion to cause any Al dissolution.

The neat epoxy film exhibited polarisation behaviour similar to that of metals corroding in a uniform manner. Sharp and sustained increases in the current density were not observed, whereas the anodic-to-cathodic transition potential was nobler than the corrosion potential. The higher current densities during reverse polarisation, as compared to those during forward polarisation, could be attributed to the water diffusion into the polymer. However, the abrupt change in the gradient of the polarisation curve (Fig. 5b) at the “breakaway” potential, as well as the negative hysteresis loop could be indicative of deviations from the uniformity of electrolyte attack. The general degradation of the neat epoxy could be explained by the two modes of water sorption into epoxy resins [35,36]: (i) sorption by the free volume of the polymer, depending on the cross-link density; and (ii) hydrogen bonding of water molecules into hydrophilic sites present in the polymer network. Deviations from the above behaviour due to localised processes could be due to the existence of regions of deficient cross-link density [37]: Pure epoxies in aqueous solutions exhibit low resistance conduction pathways, associated with areas of poor cross-link density due to solidification and curing. In neat epoxy, regions of low cross-link density can be connected throughout the structure, whilst only occupying a very low volume fraction. This process is strongly affected by stresses developed during curing and post-curing and by evaporation of volatile material. Indeed, evaporation of volatile material was observed in the investigated

epoxy systems, as demonstrated in Fig. 7. A likely anodic reaction could be the carbon dissolution at areas of low-cross link density:



It can be postulated that the cathodic current was caused by reduction of the polymer backbone [27] and the conduction pathways being present in the epoxy as aforementioned. Even assuming that some dissolution of Al had taken place through limited access of electrolyte to the substrate/polymer interface, the effective protection ability of the polymer film was still demonstrated when comparing its polarisation curve with the polarisation curve of the bare substrate: lower cathodic currents at the low cathodic potentials and substantially lower anodic currents at the high anodic potentials were generated in the case of the coated aluminium, whilst pitting corrosion was inhibited.

To summarise, the following observations governed the behaviour of the pure epoxy coating: (i) the non-detection of Al^{3+} at the substrate/neat adhesive film interface after 24 h of immersion in the electrolyte, (ii) the different shapes of polarisation curves of the uncoated and coated Al-alloy by the neat epoxy and (iii) the presence of evaporation-due porosity in the epoxy. All the above observations led to the conclusion that the polarisation behaviour of the neat epoxy film was due to water uptake by the main volume of the polymer (primarily) and areas of deficient cross-link density (secondarily) and not to Al^{3+} transport.

3.1.3. CNT doped epoxy film

As the CNT-doped film was conductive, it supported the cathodic reaction of oxygen reduction allowing the passage of electrons needed for oxygen reduction. However, the observed cathodic currents were lower than those corresponding to the bare substrate and even lower to those corresponding to the neat epoxy film. This observation suggested a limitation of the cathodic reduction. As in the case of the neat epoxy film, a likely anodic reaction could have been the carbon dissolution at polymer areas of low-cross link density.

¹ For interpretation of color in Figs. 1, 3, 6, 8, and 9 the reader is referred to the web version of this article.

In case of the CNT doped adhesive films, the shape of the forward polarisation curves (Fig. 5c and d) was similar to that of an alloy that has suffered from localised corrosion, i.e. (a) At the breakaway potential a sharp increase in the rate of current density increase was observed. The notably decreased gradient was sustained for more than one order of magnitude current density values. (b) The reverse polarisation curve formed a negative hysteresis loop that eventually led to anodic-to-cathodic transition potential that was lower than the corrosion potential. The localised degradation was associated to the existence of CNTs, since in Polymeric Matrix Composites (PMCs), water has the tendency to segregate at the reinforcement/matrix interface [38]. This segregation was further enhanced according to the following postulation: Dissolution of carbon from the polymer phase by reaction (1) resulted in an increase in the carbonate concentration. The resultant concentrated carbonate solution provoked further segregation by osmosis and probably locally attacked the epoxy network, increasing thus the free volume and allowing further water infusion at the interface [39]. Therefore, the introduction of interfaces provided another short-circuit path causing the sustained current increase at potentials greater than E_b . Similar trends in other types of CNT/epoxy coatings on Al substrates have also been reported [40].

The effect of the CNT content to localised degradation (Table 1 and Fig. 5c and d), can be summarised in the following statements: (a) The breakdown state of the 1% CNT containing surface started at a current density that was half of the respective value at the 0.5% CNT containing surface. (b) The $(E_b - E_{cor})$ value for the 1% CNT containing surface was greater than the respective value for the 0.5% CNT containing surface. (c) The $(E_{cor} - E_{a/c/tr})$ value for the 1% CNT containing surface was lower than the respective value for the 0.5% CNT containing surface. (d) The anodic (forward) curve gradient characterising the breakdown state of the 0.5% CNT containing surface was flatter than the respective gradient of the 1% CNT containing surface. Observations (b), (c) and (d) were indicative of a higher resistance against localised degradation for the 1% CNT doped film. However, observation (a) favoured the opposite. Nevertheless, the similar shapes of the polarisation curves for the two doped films suggested similar degradation mechanisms.

As is shown in Table 1, the uniform degradation rate (i_{cor}) of the three coating systems followed the order: (neat epoxy + 1% CNTs) < (neat epoxy + 0.5% CNTs) < (neat epoxy). Although the incorporation of CNTs increased the conductivity of the neat epoxy by forming a conductive percolating network [25,41], it decreased the uniform degradation rate. This observation was compatible with previous work performed in an alternative adhesive system [40]. Furthermore, the uniform degradation rate decreased with increasing CNTs content of the composite film. Thus, it was inferred that the CNTs incorporation limited the electrolyte paths in the epoxy. A plausible explanation was based on the following: Water penetration into polymer matrix composites (PMCs) involves three mechanisms [42]: (a) direct diffusion of water molecules into the matrix and, to a much less extent, into the filler material; (b) flow of water molecules along the filler–matrix interface, followed by diffusion into the bulk resin; and (c) transport of water by microcracks or other forms of , such as pores or small channels already present in the material or generated by water attack. The introduction of CNTs/matrix interfaces favours mechanism (b), thereby favouring localised degradation. As was shown in a previous study, doping epoxy matrix with CNTs led to a slight increase of approximately 0.2% on the water uptake [43]. However, at the same time CNTs can act as microcrack deflectors, limiting mechanism (c). Previous studies have demonstrated that appropriate dispersion led to enhancement of the critical stress intensity factor and the fracture toughness of the CNT modified epoxies of up to 250% compared to the values of the neat epoxy resin [12]. Mechanism (c) may also be obstructed by the blocking of microscale defects in the coating by

the nanoscale CNTs (such as the large pores observed in Fig. 7). Moreover, since the surfaces of as-grown CNTs are hydrophobic [44], they can prevent hydrogen bonding of water molecules into hydrophilic sites present in the polymer matrix.

The protection ability of the CNT doped adhesive films is illustrated in Fig. 7. Even though the coating presented a significant occurrence of pores due to volatilisation, the Al-alloy surface was absolutely free of degradation signs. Even, if some dissolution of Al had taken place through limited access of electrolyte to the substrate/composite film interface, the effective protection ability of the composite films was still evident when comparing their polarisation curve with the polarisation curve of the bare substrate: lower cathodic currents at the low cathodic potentials, substantially lower anodic currents at the high anodic potentials were generated in the case of the coated aluminium, whilst pitting corrosion was largely inhibited.

The stabilisation of current at high anodic overpotentials (Fig. 5b–d) could be attributed to the saturation of the polymer with water. As has been demonstrated for epoxy reinforced with silane coated and uncoated silicate glass microspheres (bulk systems) at various volume fractions, water uptake saturation in saturated NaCl and MgCl₂ aqueous solutions depended on various parameters, such as the reinforcement volume fraction, the activity of water and the thickness of the bulk material [37,39]. Additionally, deposition of unstable polymer oxidation products was possible [45].

To summarise, the electrochemical evidence of localised degradation, whilst the Al2024/CNT doped film interface had remained (SEM wise) intact, suggested that the polarisation behaviour of the CNT doped film in the potential range of sustained current increase was due to preferential water transport through pathways of low cross-link density and CNT/polymer matrix interfaces. Moreover, the different shapes of the polarisation curves of neat film and CNT doped film suggested that the water transport through the CNT/polymer matrix interface was the controlling mechanism for the polarisation behaviour of the CNT doped films.

3.2. Galvanic effect

Fig. 8 presents the galvanic current vs. immersion time plots for the couples: anodised Al 2024 T3- Neat epoxy, anodised Al 2024 T3-0.5% CNT doped epoxy and anodised Al 2024 T3-1.0% CNT doped epoxy. The positive values of the current density showed that the Al-alloy was anodic to the composites, in compatibility with the rest potential and corrosion potential measurements (Table 1). In other words, if the Cl⁻ ions reached the alloy substrate its

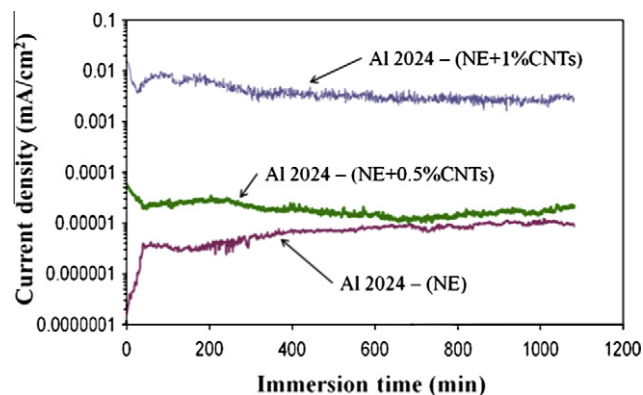


Fig. 8. Galvanic current vs. time for the couples: anodised Al 2024 T3-neat epoxy (NE), 0.5 wt.% CNT doped epoxy-anodised Al2024 T3 and (d) 1.0 wt.% CNT doped epoxy-anodised Al2024 T3 (aerated 3.5% NaCl, R.T.).

corrosion would be accelerated, as the latter was anodic to its coating. This coating arrangement was susceptible to detachment of the coating from its substrate, if the electrolyte reached the interface [46].

In the case of the Al-alloy/neat epoxy, the galvanic current values even after 18 h of immersion were very low (8.8×10^{-6} mA/cm²), indicating that the ion movement was very small and, consequently, the galvanic corrosion phenomena between the two materials were insignificant. In the case of the Al-alloy/0.5% CNT containing resin, the galvanic effect was similarly low (galvanic current after 18 h of immersion: 2.2×10^{-5} mA/cm²), although somewhat greater than that of the Al-alloy/neat epoxy system. This was attributed to the increased conductivity of the adhesive film. However, incorporation of 1.0% CNT into the polymer film notably increased the Al-alloy/0.5% CNT galvanic effect by almost two orders of magnitude (galvanic current after 18 h of immersion: 2.9×10^{-3} mA/cm²). This large increase indicated a percolation threshold of electrical conductivity greater than 0.5 wt.% CNT [47].

As can be seen in Fig. 8, the current oscillations of the current density vs. time curves indicate deposition of instable corrosion products, pit formation on Al2024 and repassivation. In the case of the Al-0.5% CNT doped epoxy, the slightly increasing trend of current density after ~10 h of immersion suggested a tendency towards stable pitting.

However, the most important observation was that the presence of the CNTs did not mediate the effects of the galvanic corrosion. This is in compatibility with previous work [40], where 0.1% CNT inclusion in CFRPs, had also increased the galvanic effect between the substrate and the patch albeit a much less extent. 0.1% CNTs incorporation had resulted in doubling the galvanic current of the substrate/adhesive film couple although the measured galvanic currents of the couple Al alloy/1.0% CNTs doped CFRPs were one order of magnitude higher than the ones measured in the present work. Hence, it is inferred that the corrosion behaviour of these materials is system (type of adhesive, hardener and reinforcement) dependent. Another factor crucial for the galvanic effect determination of the couple Al alloy/adhesive coating is the surface state of the substrate, as far as the quality of the cathodic film is concerned. A sufficiently sealed film would probably change the conductivity of the immersed alloy and, hence, the galvanic effect of the studied couples. The effect of the quality of the cathodic film on the galvanic effect of the substrate/patch couple is currently under investigation.

Nevertheless, a very interesting result was that the CNT incorporation in the adhesive film led to decreased rates of general corrosion (considered proportional to the corrosion current densities) and also slightly nobler surfaces regarding the corrosion potential and the rest potential values (Table 1). At the same time, it was shown that the doped film effectively protected the Al-alloy during cyclic polarisation. Therefore, it can be assumed that a bi-layer patch, where the intermediate layer will be the neat polymer film (which was compatible with the Al-substrate in terms of galvanic corrosion, as Fig. 8 suggests) and the over-layer will be the CNT-reinforced film (which exhibited relatively low uniform degradation rate), might be beneficial in terms of corrosion protection of the Al-alloy. The same conclusion was previously reached for a different type of polymer system [40]. In that study, the CNTs-doped film exhibited distinctly superior potentiodynamic polarisation behaviour as compared to the neat CFRP film, regarding not only the corrosion current densities but also the corrosion potential, the rest potential and the generated currents in general. Hence, it is once more inferred that the corrosion behaviour of CNTs doped polymers and PMCs is system dependent. This observation may be closely related to the fact that the electrical conductivity of PMCs with identical filler concentrations has been reported to vary by 10 or more orders of magnitude for different matrices [41]. In his

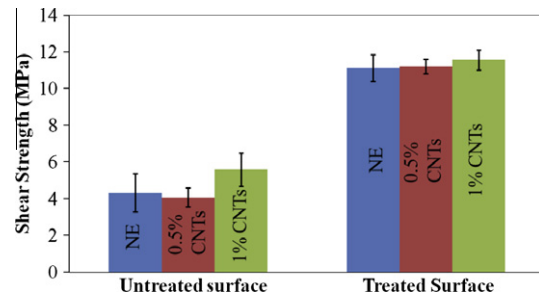


Fig. 9. Lap shear strength for both treated and untreated aluminium substrates.

respect, although the percolation threshold dominates the galvanic behaviour, the CNTs can be a suitable medium which with controlled loading and dispersion may serve as a corrosion control medium in order to allow the application of carbon fibre reinforced composites in patch repair.

3.3. Adhesion enhancement with CNT incorporation

In Fig. 9, the adhesive bonded strength for plain and CNT modified adhesive is depicted as the average of five specimens. The large majority of the specimens failed in an adhesive mode. As can be seen, surface treatment was critical to the adhesion efficiency.

The incorporation of the CNTs enhanced adhesion in all but one case. As is well known, the surface topography plays an important role in adhesion because pits, valleys, peaks and other types of topographical features on the surfaces of the adherents provide additional surface area for bonding and allows for mechanical interlocking to take place between the substrate and adhesive, enhancing adhesion [48,49]. Conversely, surfaces with very high peaks or deep holes may allow for air to be trapped at the interfaces, creating stress concentrations in the interface region of the bond and compromising adhesion.

The enhancement of the adhesion was significant in the case of untreated substrate and 1% CNTs modified adhesive. In this case, the adhesion enhancement reached almost 50% compared to the unmodified and 0.5% CNTs modified epoxy. A typical *T*-test in order to assess the significance of the improvement showed that the 0.5% doped system performs better at least at a confidence level of 99.5% (yielding $t = 3.17$, larger than $t_{99.5} = 2.80$ for 24 degrees of freedom). The large experimental scatter was attributed to variations due to the manually sanded surface and not directly to the CNT incorporation. The considerable adhesion enhancement may be attributed to the CNTs/epoxy interface which activated mechanisms at the nanoscale such as crack bifurcation and arrest, delaying thus the global shear failure [8]. Interestingly enough, the enhancement was only observed for 1% CNT, indicating that adhesion improvement was becoming statistically significant after a critical loading.

As can be seen in Fig. 9, adhesion improved spectacularly (in some cases tripled) with the anodising process. For the treated (anodised) Al 2024 T3, the improvement achieved with the incorporation of CNTs was by far less (approximately 4%). The *T*-test comparing plain and 1% CNT samples yields that improvement is significant only at 95% confidence level, but not at 97.5%. Generally, the adhesion enhancement provided by the CNTs was masked by the effect of the anodising process.

4. Conclusions

This work involved the incorporation of CNTs in aerospace structural adhesive with a view (a) to assess the electrochemical

behaviour of the modified adhesive layer and (b) investigate the effect of the CNTs reinforcement to the adhesion efficiency of the structural adhesive.

The incorporation of CNTs retarded or even inhibited the electrolyte progress towards the substrate surface. This was attributed to the CNTs acting as microcrack deflectors and/or preventing hydrogen bonding of water molecules into hydrophilic sites of the polymer matrix. The galvanic effect of the modified adhesive was governed by the percolation threshold of the CNTs in the epoxy.

The CNTs incorporation resulted to approximately 50% enhanced adhesion efficiency compared to the neat and 0.5% doped adhesive, albeit with significant experimental scatter. Surface treatment of the adherents proved to be critical in enhancing the adhesion efficiency providing additional surface area for bonding and enhancing adhesion. The effect of additional surface treatment (in this case was standard anodising) proved to be much more pronounced masking the beneficial effect rising from the incorporation of the CNTs.

Summarising, CNTs when employed as additives in typical aerospace adhesives were found to be very promising in both (i) tailoring the galvanic behaviour of nanocomposites and (ii) enhancing their adhesion efficiency. In this respect, they may be employed as a reinforcing/mediation phase in order to allow the widespread use of bonded repair with carbon fibre reinforced composites.

Acknowledgements

The authors would like to acknowledge the EU (IAPETUS PROJECT, Grant Agreement Number: ACP8-GA-2009-234333) for financial support and Dr. A.E. Karantzalis for his contribution regarding Scanning Electron Microscopy.

References

- Baker AA. Joining and repair of aircraft composite structures. In: Mallick PK, editor. Composite Engineering Handbook. New York: Marcel Decker Inc.; 1997. p. 671–776.
- Yu S, Tong MN, Critchlow G. Use of carbon nanotubes reinforced epoxy as adhesives to join aluminium plates. Mater Des 2010;31 [Supplement 1(0):S126–S9].
- Balzani C, Wagner W, Wilckens D, Degenhardt R, Büsing S, Reimerdes HG. Adhesive joints in composite laminates—a combined numerical/experimental estimate of critical energy release rates. Int J Adhes Adhes 2012;32:23–38.
- Campbell FC. Manufacturing processes for advanced composites. Kidlington, Oxford, United Kingdom: Elsevier Ltd.; 2004.
- Baker AA, Roberts JD, Rose LRF. Experimental study of overlap joint parameters relevant to the K reduction due to crack-patching. In: National SAMPE symposium and exhibition (proceedings), SAMPE, Azusa, CA, USA, 1983. p. 627–39.
- Baker AA, Chester RJ. Recent advances in bonded composite repair technology for metallic aircraft components. In: Chandra T, Dhingra AK, (editors). Proceedings of the international conference on advanced composite materials, Wollongong, Australia, 15–19 February 1993. Publ by Minerals, Metals & Materials Soc (TMS), Warrendale, PA, United States, 1993. p. 45–9.
- Karapappas P, Vavouliotis A, Tsotra P, Kostopoulos V, Paipetis A. Enhanced fracture properties of carbon reinforced composites by the addition of multi-wall carbon nanotubes. J Compos Mater 2009;43:977–85.
- Kostopoulos VTS, Fanis N. Tension–tension fatigue behaviour of carbon nanotube doped carbon unidirectional fibre reinforced epoxy composites. ECCM 11, Rodos, Greece; 2004.
- Kostopoulos V, Tsotra P, Karapappas P, Tsantzalis S, Vavouliotis A, Loutas TH, et al. Mode I interlaminar fracture of CNF or/and PZT doped CFRPs via acoustic emission monitoring. Compos Sci Technol 2007;67:822–8.
- Kostopoulos V, Baltopoulos A, Karapappas P, Vavouliotis A, Paipetis A. Impact and after-impact properties of carbon fibre reinforced composites enhanced with multi-wall carbon nanotubes. Compos Sci Technol 2010;70:553–63.
- Srivastava VK. Effect of carbon nanotubes on the strength of adhesive lap joints of C/C and C/C–SiC ceramic fibre composites. Int J Adhes Adhes 2011;31:486–9.
- Gkikas G, Barkoula NM, Paipetis AS. Effect of dispersion conditions on the thermo-mechanical and toughness properties of multi walled carbon nanotubes-reinforced epoxy. Compos Part B: Eng.
- Montazeri A, Khavandi A, Javadpour J, Tcharkhtchi A. Viscoelastic properties of multi-walled carbon nanotube/epoxy composites using two different curing cycles. Mater Des 2010;31(7):3383–8.
- Gojny FH, Wichmann MHG, Fiedler B, Schulte K. Influence of different carbon nanotubes on the mechanical properties of epoxy matrix composites—A comparative study. Compos Sci Technol 2005;65:2300–13.
- Kim YJ, Shin TS, Choi HD, Kwon JH, Chung Y-C, Yoon HG. Electrical conductivity of chemically modified multiwalled carbon nanotube/epoxy composites. Carbon 2005;43:23–30.
- Jana S, Zhong W-H, Gan YX. Characterisation of the flexural behaviour of a reactive graphitic nanofibers reinforced epoxy using a non-linear damage model. Mater Sci Eng A 2007;445–446:106–12.
- Montazeri A, Javadpour J, Khavandi A, Tcharkhtchi A, Mohajeri A. Mechanical properties of multi-walled carbon nanotube/epoxy composites. Mater Des 2010;31(9):4202–8.
- Wichmann MHG, Schulte K, Wagner HD. On nanocomposite toughness. Compos Sci Technol 2008;68:329–31.
- Li Q, Dong L, Li L, Su X, Xie H, Xiong C. The effect of the addition of carbon nanotube fluids to a polymeric matrix to produce simultaneous reinforcement and plasticisation. Carbon 2012.
- de la Vega A, Kovacs JZ, Bauhofer W, Schulte K. Combined Raman and dielectric spectroscopy on the curing behaviour and stress build up of carbon nanotube–epoxy composites. Compos Sci Technol 2009;69:1540–6.
- Buchheit RG. Compilation of corrosion potentials reported for intermetallic phases in aluminium alloys. J Electrochem Soc 1995;142:3994–6.
- Buchheit RG, Grant RP, Hlava PF, McKenzie B, Zender GL. Local dissolution phenomena associated with S phase (Al₂CuMg) particles in aluminium alloy 2024–T3. J Electrochem Soc 1997;144:2621–8.
- Reynolds LB, Twite R, Khobaib M, Donley MS, Bierwagen GP. Preliminary evaluation of the anticorrosive properties of aircraft coatings by electrochemical methods. Prog Org Coat 1997;32:31–4.
- Foley RT. Localised corrosion of aluminium alloys – a review. Corrosion 1986;42:277–88.
- Ireland R, Arronche L, La Saponara V. Electrochemical investigation of galvanic corrosion between aluminum 7075 and glass fiber/epoxy composites modified with carbon nanotubes. Compos Part B: Eng 2012;43(2):183–94.
- Chen XH, Chen CS, Xiao HN, Cheng FQ, Zhang G, Yi GJ. Corrosion behaviour of carbon nanotubes–Ni composite coating. Surf Coat Technol 2005;191:351–6.
- Angelopoulos M. Conducting polymers in microelectronics. IBM J Res Dev 2001;45:57–75.
- ASTM Standard D3933. Standard guide for preparation of aluminum surfaces for structural adhesives bonding (phosphoric acid anodizing). ASTM International, West Conshohocken, PA, 1998. doi:10.1520/D3933-98.
- Lekatou A, Zois D, Karantzalis AE, Grimanellis D. Electrochemical behaviour of cermet coatings with a bond coat on Al7075: pseudopassivity, localised corrosion and galvanic effect considerations in a saline environment. Corros Sci 2010;52:2616–35.
- ASTM Standard D5868. Standard test method for lap shear adhesion for fiber reinforced plastic (FRP) bonding. ASTM International, West Conshohocken, PA, 1995. doi: 10.1520/D5868-95.
- Altenpohl DG. Aluminium: technology, applications, and environment: a profile of a modern metal. 6th ed. TMS, Warrendale, Pennsylvania; 1998.
- Bond AP, Bolling GF, Domian HA, Biloni H. Microsegregation and the tendency for pitting corrosion in high-purity aluminium. J Electrochem Soc 1966;113(8):773–8.
- Stansbury EE, Buchanan RA. Fundamentals of electrochemical corrosion. 1st ed. ASM International, Materials Park, OH; 2000. p. 328.
- Clark RA, Krueger GL. Aluminon - its limited application as a reagent for the detection of aluminum species. J Histochem Cytochem 1985;33:729–32.
- Apicella Aa N. Advances in polymer science 72: epoxy and resins, vol. 6. Springer-Verlag, Berlin, 1985, p. 70.
- Apicella A, Egiziano L, Nicolais L, Tucci V. Environmental degradation of the electrical and thermal properties of organic insulating materials. J Mater Sci 1988;23:729–35.
- Lekatou A, Faidi SE, Ghidaoui D, Lyon SB, Newman RC. Effect of water and its activity on transport properties of glass/epoxy particulate composites. Compos A Appl Sci Manuf 1997;28:223–36.
- Hull D. An introduction to composite materials. Camb Sol State Sci Ser, Cambridge University Press, UK; 1981.
- Lekatou Sef A, Lyon SB, Newman RC. Elasticity and fracture in particulate composites with strong and degraded interfaces. J Mater Res 1996;11:1293–304.
- Gkikas G, Lekatou A, Barkoula NM, Sioulas D, Canflanca B, Florez S, et al. Corrosion Int J Structural Integrity 2011.
- Bauhofer W, Kovacs JZ. A review and analysis of electrical percolation in carbon nanotube polymer composites. Compos Sci Technol 2009;69:1486–98.
- Marom G. The role of water transport in composite materials. J Comyn (Ed.), Polymer Permeability, Elsevier Applied Science Publishers, London/New York, 1985, p. 341–73.
- Barkoula NM, Paipetis A, Matikas T, Vavouliotis A, Karapappas P, Kostopoulos V. Environmental degradation of carbon nanotube-modified composite laminates: a study of electrical resistivity. Mech Compos Mater 2009;45:21–32.
- Tzeng Tsh Y, Chen YC, Liu C, Liu YK. Hydration properties of carbon nanotubes and their effects on electrical and bio-sensor applications. New Diamond Front. Carbon Technol. 2004;14:193–201.
- Billingham NC. Degradation and stabilisation of polymers. Mater Sci Technol: A Compr Treat: Wiley-VCH Verlag GmbH; 2008. p. 469–507.

- [46] Guilemany JM, Dosta S, Miguel JR. The enhancement of the properties of WC-Co HVOF coatings through the use of nanostructured and microstructured feedstock powders. *Surf Coat Technol* 2006;201:1180–90.
- [47] Yuen S-M, Ma C-CM, Wu H-H, Kuan H-C, Chen W-J, Liao S-H, et al. Preparation and thermal, electrical, and morphological properties of multiwalled carbon nanotube and epoxy composites. *J Appl Polym Sci* 2007;103:1272–8.
- [48] Chin JW, Wightman JP. Surface characterisation and adhesive bonding of toughened bismaleimide composites. *Compos Part A Appl Sci Manuf* 1996;27:419–28.
- [49] Packham DE. Surface energy, surface topography and adhesion. *Int J Adhes Adhes* 2003;23:437–48.